Epidemic spreading and risk perception in multiplex networks: A self-organized percolation method

Emanuele Massaro[*]
Risk and Decision Science Team, US Army Engineer Research and Development Center, 696 Virginia Road, Concord, Massachusetts 01742 and Department of Civil and Environmental Engineering, Carnegie Mellon University, 5000 Forbes Avenue, Pittsburgh, Pennsylvania 15213, USA

Franco Bagnoli[†]
Dipartimento di Fisica e Astronomia and CSDC, Università degli Studi di Firenze, and INFN, Sezione di Firenze, via G. Sansone 1, 50019 Sesto Fiorentino, Firenze, Italy
(Received 22 May 2014; published 18 November 2014)

In this paper we study the interplay between epidemic spreading and risk perception on multiplex networks. The basic idea is that the effective infection probability is affected by the perception of the risk of being infected, which we assume to be related to the fraction of infected neighbors, as introduced by Bagnoli *et al.* [Phys. Rev. E **76**, 061904 (2007)]. We rederive previous results using a self-organized method that automatically gives the percolation threshold in just one simulation. We then extend the model to multiplex networks considering that people get infected by physical contacts in real life but often gather information from an information network, which may be quite different from the physical ones. The similarity between the physical and the information networks determines the possibility of stopping the infection for a sufficiently high precaution level: if the networks are too different, there is no means of avoiding the epidemics.

DOI: 10.1103/PhysRevE.90.052817 PACS number(s): 64.60.aq, 05.65.+b

I. INTRODUCTION

Recently, *Health* magazine reported, "Although H1N1 influenza killed more than 4,000 people in the United States in 2009–2010, this outbreak was relatively mild compared to some flu pandemics" [1]. Indeed, the twentieth century was characterized by a series of more serious events. During 1918–1919 the world was involved in the so-called Spanish flu. Starting in three places: Brest (France), Boston (Massachusetts, USA), and Freetown (Sierra Leone), the disease spread worldwide, killing 25 million people in 6 months (about 17 million in India, 500 000 in the United States, and 200 000 in the United Kingdom).

In 1957, another pandemic originated in China and spread rapidly in Southeast Asia, hence taking the name Asian flu. The virus responsible was identified as subtype H2N2, new to humans, resulting from a previous human H1N1 virus that was remixed with a duck virus from which it received the genes encoding H2 and N2. This pandemic took 8 months to travel worldwide and took 1 million to 2 million victims.

The 1968 pandemic was the mildest of the twentieth century and started, once again, in China. From there it spread to Hong Kong, where more than half a million people fell ill, and in the same year it reached the United States and the rest of the world.

Given these facts (and the entire record of pandemics throughout history [2]), it is not surprising that public health organizations are concerned about the appearance of a new deadly pandemic. However, in recent decades there have been many cases of false or exaggerated information about epidemics. Examples are the swine flu of 1976; the avian flu of 1997, where a United Nations health official warned that the virus could kill up to 150 million worldwide [1]; and the more recent 2009 H1N1 flu, during whose outbreak the U.K. Department of Health warned of about 65 000 possible deaths as reported by the *Daily Mail* in 2010 [3]. Fortunately, these fears did not realize.

These catastrophic scenarios and the extent of their impact in economic and social contexts induce reflection on the method used to forecast the evolution of a disease in the real world. It is well known that in deeply connected networks (in particular, in scale-free ones without strong compartmentalization), the epidemic threshold of standard epidemic modeling is vanishing [4–8]. Indeed, the *lazzarettos* [9] experience, first in Venice and then in many ports and cities, was so successful in the absence of effective treatments because it was able to break the contact network. The pest was last observed in Venice in 1630, whereas in southeastern Europe, it was present until the nineteenth century [10].

However, the last deadly pest pandemics occurred in Europe in 1820 [2] and, worldwide, in Vietnam in the 1960s; the last pandemic influenza, Hong Kong flu, in 1968–1969. In other words, the last rapid deadly pandemics happened well before the appearance of highly connected human networks.

Clearly, public health systems have put a lot of effort into trying to make people aware of the dangers connected with poor hygiene, dangerous sexual habits, and so on. Indeed, the current worldwide diffusion of large-scale diseases (HIV, seasonal influenza, cold, papilloma virus, herpes virus, and viral hepatitis, among others) is deeply related to their silent (and slow) progression or to the assumption (possibly erroneous) of their harmlessness. However, it is well known that direct experience (contact with actual ill people) is much more influential than public exhortations.

Therefore, in order to accurately model the spreading of a disease in human societies, we need to take into account the perception of its impact and the consequent precautions that people take when they become aware of an epidemic.

[*]emassaro@andrew.cmu.edu
[†]franco.bagnoli@unifi.it

These precautions may consist in changes in personal habits, vaccination, or modifications of the contact network.

We are interested here in diseases for which no vaccination is possible (or performed), so that the only way to avoid a pandemic is by means of an appropriate level of precautions, in order to lower the infection rate below the epidemic threshold. We also assume that there is no acquired immunity from the disease and that its consequences are neglected so that they do not induce any radical change in social contacts or reach the mass media level. Indeed, one of the dangers of this negligence is the sudden outbreak of epidemics, as we show in the following.

In a previous work [11], some of us investigated the influence of risk perception in epidemic spreading. We assumed that knowledge about the diffusion of the disease among neighbors (without knowing who is actually infected) effectively lowers the probability of transmission (the effective infectiousness). We studied the worst case of an infection on a scale-free network with exponent $\gamma = 2$ and we showed that in this case no degree of prevention is able to stop the infection and one has to take additional precaution for hubs (such as public officers and physicians).

Here we extend the investigation to different network structures, in order to obtain a complete reference frame. For regular, random, Watts-Strogatz small-world, and nonassortative scale-free networks with exponent $\gamma > 3$, there is always a finite level of precaution parameter at which the epidemics go extinct. For scale-free networks with $\gamma < 3$ the precaution level depends on the cutoff of the power law, which depends at least on the finite number of the nodes of the given network.

We consider, then, an important factor of modern society: the fact that most of the information comes not from physical contacts nor from broadcasting media but, rather, from the "virtual" social contact networks [12–14]. A series of recent studies on the "State of the News Media" in the United States [15] highlights this phenomenon. It shows the extent of the influence of social networks, for subscribers who can read news published in newspapers. The 9% of this population claims to inquire "very often" through Facebook and Twitter and the 70% of newspaper subscribers on Facebook are referred to articles (from newspapers and other sources) by friends and family members who are in any case the main drivers of news.

We are therefore confronted with news coming mainly from an information network. On the other hand, the physical network of contacts is the environment in which actual infections occur. We consider diseases that have few or no visible symptoms, so that the only way to get information about them is by effective information sharing. However, one generally does not share information (e.g., talk) with all of his or her physical contacts. It may happen that one gets infected, say, on a public transportation system by an unknown person who belongs to his or her effective physical contact network but not to his or her information network.

We therefore extend our model to the case in which the source of information (mixed physical and virtual contacts) does not coincide with the actual source of infection (the physical contacts). This system is well represented as a multiplex network [16–20], i.e., a graph composed of several layers in which the same set of N nodes can be connected to each other by means of links belonging to different layers, which represents a specific case of the interdependent network [21,22]. Recently, Granell *et al.* [23] have drawn attention to an interesting scenario in which the multiplex corresponds to a two-layer network, one where the dynamics of the awareness about the disease (the information dynamics) evolves and another where the epidemic process spreads. Recently they have also investigated the effect of mass media when all the agents are aware of the infection [24], which is the best case for stopping the epidemic. However, here we are interested in studying the case of neglected diseases, where the probability of being aware of the disease is very low.

The first layer represents the information network, where people become aware of the epidemic thanks to news coming from virtual and physical contacts in various proportions. The second layer represents the physical contact network, where epidemic spreading takes place.

In this paper we want to model the effect of virtual information on simulating the awareness of the agents in real-world network contacts. We study how the percolation threshold of susceptible-infected-susceptible (SIS) dynamics depends on the perception of the risk (which affects the infectivity probability) when this information comes from the same contact network of the disease or from a different network. In other words, we study the interplay between risk perception and spreading of disease in multiplex networks.

We are interested in the epidemic threshold, which is a quantity that it is not easy to obtain automatically (for different values of the parameters) using numerical simulations. We extend a self-organized formulation of percolation phenomena [25] that allows us to obtain this threshold in just one simulation (for a sufficiently large system).

II. THE NETWORK MODEL

In this section we report our method for generating multiplex networks. First, we describe the mechanisms for generating *regular*, *random*, and *scale-free* networks.

Let us denote by $a_{ij} = 0,1$ the adjacency matrix of the network, $a_{ij} = 1$ if there is a link from j to i and $a_{ij} = 0$ otherwise. We denote by $k_i = \sum_j a_{ij}$ the connectivity of site i and by $j_1^{(i)}, j_2^{(i)}, \ldots, j_{k_i}^{(i)}$ that of its neighbors ($a_{i,j_n^{(i)}} = 1$). We consider only symmetric networks. We generate networks with N nodes and $2mN$ links, so that the average connectivity of each node is $\langle k \rangle = 2m$.

(i) Regular one-dimensional: Nodes are arranged in a ring (periodic boundary condition). Any given node establishes a link with the m closest nodes on its right. For instance, for $m = 2$, node 1 establishes a link with nodes 2 and 3, node 2 with nodes 3 and 4, and so on, until node $N - 1$ establishes links with nodes N and 1 and node N with nodes 1 and 2.

(ii) Random: Any node establishes m links with randomly chosen nodes, avoiding self-loops and multiple links. The probability distribution of random networks is Poissonian, $P(k) = \frac{z^k e^{-z}}{k!}$, where $z = \langle k \rangle$.

(iii) Scale-free: We use a configurational model also fixing a cutoff K. First, at each node i is assigned a connectivity k_i draft from a power-law distribution $P(k) = Ak^{-\gamma}$, $m \leqslant k \leqslant K$, with $A = (\gamma - 1)/(m^{1-\gamma} - K^{1-\gamma})$. Then links are

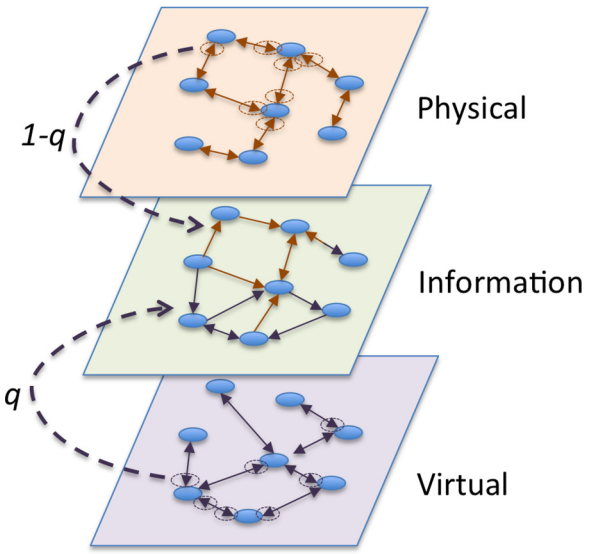

FIG. 1. (Color online) Example of a multiplex generated with our method. We start with the physical and the virtual networks, both symmetric and with the same average connectivity, and then we build the information network by choosing, for each node, outgoing links with probability q from the virtual network and with probability $1-q$ from the real network.

connected at random, avoiding self-loops and multiple links, and finally, the total number of links is pruned in order to adjust the total number of links. This mechanism allows us to generate scale-free networks with a given exponent γ.

We are interested in multiplex networks composed of two layers that we denote *physical* and *information*. First, we generate the physical network by choosing one from the regular, random, or scale-free group. Then we generate a *virtual* network also chosen from the three benchmark networks, with the same average connectivity $\langle k\rangle = 2m$. In order to construct the information network, for each node we add outgoing links from the physical network with probability $1-q$ and links from the virtual network with probability q. Since this process is repeated independently for each node, the resulting information network is no longer symmetric (a given link can be chosen by one of its vertices but not by the other). The quantity $Nq\langle k\rangle$ corresponds to the difference between the information and the physical network.

This procedure allows us to study the effects of the difference between the physical network, where epidemic spreading takes place, and the information one, where actors become aware of the disease, i.e., over which they evaluate the perception of the risk of being infected. An example of a multiplex is shown in Fig. 1.

III. INFECTION MODEL AND MEAN-FIELD APPROXIMATION

Following Ref. [11], we assume that the probability that a site i with connectivity i is infected by any one of s infected neighbors is given by

$$u(s,k_i) = \tau \exp\left(-J\frac{s}{k_i}\right), \tag{1}$$

where τ is the "bare" infection probability and s is the number of infected neighbors. The idea is that the perception of the risk, given by the percentage of infected neighbors and modulated by the factor J, effectively lowers the infection probability (for instance, because people take more precautions). In the case of information networks, the perception is computed in the mixed physical-virtual neighborhood, while the actual infection process takes places in the physical network.

It is possible to derive a simple mean-field approximation for the fixed-k case. Denoting by c the fraction of infected individuals at time t, and by c' that at time $t+1$, we have, considering a random network,

$$c' = \sum_{s=0}^{k}\binom{k}{s}c^s(1-c)^{k-s}p(s,k), \tag{2}$$

where $p(s,k)$ is the probability of being infected if there are s of k infected neighbors. The probability p depends on u as

$$p(s,k) = 1-[1-u(s,k)]^s,$$

since the infection processes are independent, although the infection probabilities are coupled by the "perception"-dependent infection probability q, Eq. (1).

Near the infection-percolation threshold, the probability u is low, and therefore we can approximate

$$p(s,k) \simeq su(s,k) = s\tau\exp\left(-J\frac{s}{k}\right).$$

Replacing p in Eq. (2), we get

$$c' = \sum_{s=0}^{k}\binom{k}{s}c^s(1-c)^{k-s}s\tau\exp\left(-J\frac{s}{k}\right),$$

and setting $a = \exp(-J/k)$,

$$c' = \tau\sum_{s=0}^{k}\binom{k}{s}c^s(1-c)^{k-s}sa^s,$$

which gives

$$c' = \tau ak(ca+1-c)^{k-1}.$$

The critical threshold J_c corresponds to the stationary state $c'=c$ in the limit $c\to 0$, i.e.,

$$\tau = \frac{1}{k}\exp\left(\frac{J_c}{k}\right), \quad J_c = k\ln(k\tau). \tag{3}$$

This prediction is quite accurate: in the comparison between Eq. (3) and actual simulations is reported in Fig. 2 for different values of $\langle k\rangle$ using random networks.

The analysis can be extended to nonhomogeneous networks with a connectivity distribution $P(k)$ like the scale-free ones. We can start by analyzing a node with connectivity k,

$$c'_k = \sum_{s_1,s_2,\ldots,s_k=0}^{1}\ \sum_{j_1,j_2,\ldots,j_k=0}^{\infty}\ \prod_{i=1}^{k}C(j_i,k)I(s_i,j_i)T(k|s_i),$$

where we denote by $i=1,\ldots,k$ the neighbors, $s_i=0,1$ is their state (healthy, infected), and j_i their connectivity. $C(j,k)$ is the probability that a node with connectivity j is attached to a node with connectivity k, $I(s_i,j_i)$ is the probability that

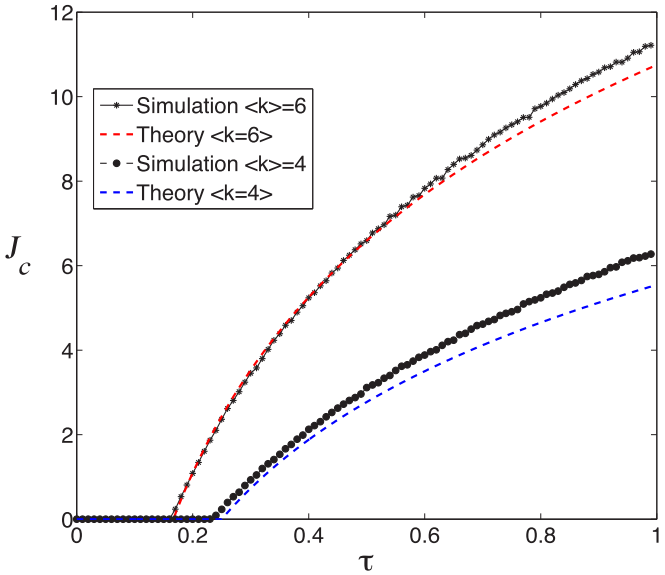

FIG. 2. (Color online) Comparison between mean-field approximation and simulations for random networks with different values of $\langle k\rangle$.

the neighbor i is infected, and $T(k|s_i)$ is the probability that it transmits the infection to the node under investigation.

Clearly, $\sum_j C(j,k) = 1$. We use symmetric networks, so $jC(j,k)P(j) = kC(k,j)P_k$ (detailed balance). For nonassortative networks, $C(j,k)$ does not depend on k, and summing over the detailed balance condition we get $C(j,k) = jP(j)/\langle k\rangle$.

The quantity $I(s_i,j_i)$ is simply $c_{j_i}^{s_i}(1-c_{j_i})^{1-s_i}$ and $T(k|s_i) = 1-(1-\tau\exp(-Js/k))^s$, where $s = \sum_i s_i$ (risk perception). Near extinction, again $\tau\exp(-Js/k)$ is small and we can approximate $T(k|s_i) = s\tau\exp(-Js/k)$.

Summing up, we have

$$c_k' = \sum_{s_1,s_2,\ldots,s_k=0}^{1}\sum_{j_1,j_2,\ldots,j_k=0}^{\infty}\prod_{i=1}^{k}\frac{j_iP(j_i)}{\langle k\rangle}c_{j_i}^{s_i} \times (1-c_{j_i})^{1-s_i}s\tau\exp\left(-J\frac{s}{k}\right) = \sum_{s_1,s_2,\ldots,s_k=0}^{1} s\tau\exp\left(-J\frac{s}{k}\right)\prod_{i=1}^{k}\sum_{j_i=0}^{\infty}\frac{j_iP(j_i)}{\langle k\rangle}c_{j_i}^{s_i}(1-c_{j_i})^{1-s_i}.$$

Let us define $\tilde{c} = \sum_j jP(j)c_j/\langle k\rangle$. Since $s_i = 0$ or 1, the quantity $c_{j_i}^{s_i}(1-c_{j_i})^{1-s_i}$ is either c_i or $1-c_i$, so that, for a given combination of $\{s_1,s_2,\ldots,s_k\}$, the sum over j_i is given by terms of the type $\sum_{j_i} j_iP(j_i)c_{j_i}/\langle k\rangle = \tilde{c}$ or $\sum_{j_i} j_iP(j_i)(1-c_{j_i})/\langle k\rangle = 1-\tilde{c}$. We can therefore say that

$$\prod_{i=1}^{k}\sum_{j_i=0}^{\infty}\frac{j_iP(j_i)}{\langle k\rangle}c_{j_i}^{s_i}\left(1-c_{j_i}\right)^{1-s_i} = \prod_{i=1}^{k}\tilde{c}^{s_i}(1-\tilde{c})^{1-s_i},$$

and thus, since $\tilde{c}$ does not depend on i,

$$c_k' = \sum_{s_1,s_2,\ldots,s_k=0}^{1} s\tau\exp\left(-J\frac{s}{k}\right)\prod_{i=1}^{k}\tilde{c}^{s_i}(1-\tilde{c})^{1-s_i} = \sum_{s=0}^{k}\binom{k}{s}s\tau\exp\left(-J\frac{s}{k}\right)\tilde{c}^s(1-\tilde{c})^{k-s};$$

i.e.,

$$c_k' = \tilde{c}k\tau\exp\left(\frac{-Js}{k}\right)\left(\tilde{c}\exp\left(-\frac{J}{k}\right)+1-\tilde{c}\right).$$

Near the epidemic threshold, $\tilde{c}\to 0$ and

$$\tilde{c}' = \frac{1}{\langle k\rangle}\sum_k kc_k'P(k) = \frac{\tau\tilde{c}}{\langle k\rangle}\sum_k k^2P(k)\exp\left(-\frac{J}{k}\right).$$

The correspondence between τ_c and J_c is therefore

$$\tau_c(J_c) = \frac{\langle k\rangle}{\sum_k k^2P(k)\exp\left(-\frac{J_c}{k}\right)}, \tag{4}$$

which, for $J_c = 0$, gives the usual relationship $\tau_c = \langle k\rangle/\langle k^2\rangle$; for a sharply peaked $P(k)$ this corresponds to Eq. (3).

By using a continuous approximation, it is possible to make explicit the relationship between τ and J_c in the scale-free case. Equation (4) becomes

$$\tau_c(J_c) = \frac{\langle k\rangle}{\int_m^K k^2P(k)\exp\left(-\frac{J_c}{k}\right)\,\mathrm{d}k}. \tag{5}$$

Substituting, for the scale-free case, $P(k) = Ak^{-\gamma}$, where A is the normalization constant so that $\int_m^K P(k) = 1$,

$$A = \frac{\gamma-1}{m^{1-\gamma}-K^{1-\gamma}} \simeq (\gamma-1)m^{\gamma-1},$$

if $K \gg m$ (and $\gamma < 3$). We get

$$\langle k\rangle = \frac{\gamma-1}{\gamma-2}\frac{m^{2-\gamma}-K^{2-\gamma}}{m^{1-\gamma}-K^{1-\gamma}} \simeq \frac{\gamma-1}{\gamma-2}m$$

for $K \gg m$, and

$$\tau_c(J_c) = J_c^{3-\gamma}\left[\Gamma\left(\gamma-3,\frac{J_c}{K}\right)-\Gamma\left(\gamma-3,\frac{J_c}{m}\right)\right], \tag{6}$$

where $\Gamma(a,x)$ is the incomplete Γ function. Equation (6) diverges for $K\to\infty$, and thus for infinite networks $J_c = 0$ $\forall\tau$. However, real networks always have a cutoff (at least due to the finite number of nodes) [26]. For $J_c = 0$ we recover the standard threshold,

$$\tau_c(0) = \frac{\gamma-3}{\gamma-2}\frac{m^{2-\gamma}-K^{2-\gamma}}{m^{3-\gamma}-K^{3-\gamma}} \simeq \frac{3-\gamma}{\gamma-2}\frac{m^{2-\gamma}}{K^{3-\gamma}}. \tag{7}$$

The problem of the epidemic threshold in finite-size scale-free networks was studied in Ref. [27]. The conclusion there is that even in finite-size networks the epidemic is hard to stop. Indeed, we find numerically that the epidemic always stops in finite scale-free networks, although the required critical value of J_c may be quite large.

In Fig. 3 the comparison between the mean-field prediction, Eq. (4), and actual simulations is shown for three instances of a scale-free network generated with the same parameters. The theoretical prediction coincides with the simulations only

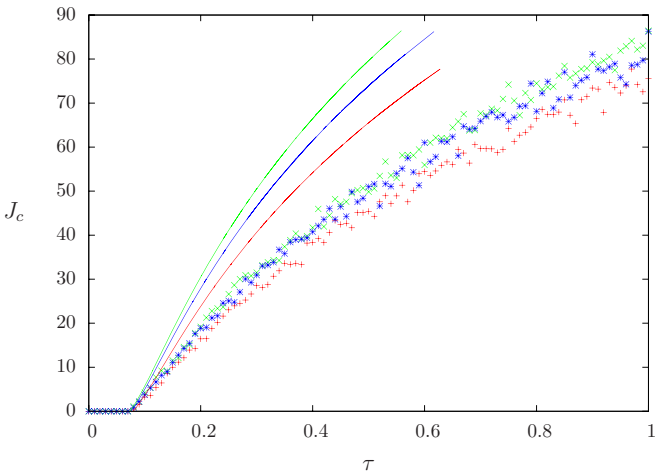

FIG. 3. (Color online) Comparison between results of the mean-field approximation (curves) and results of simulations (symbols) for three instances of scale-free networks with $\gamma = 2.4$, $N = 10\,000$, $m = 2$, and $K = 300$. Although the simulations give similar results, the mean-field computations (that coincide with the simulation only for $J_c = 0$) are very dependent on the details of the network.

for $J_c = 0$. Moreover, although the simulation result seems to be sufficiently independent of the details of the generated networks, the theoretical prediction is quite sensitive to them. The continuous approximation, Eq. (7), gives, for $m = 2$, $K = 300$, and $\gamma = 2.4$, a value of $\tau(0) \simeq 0.037$, quite different from the computed one, $\tau(0) \simeq 0.08$.

IV. THE SELF-ORGANIZED PERCOLATION METHOD

Here we report a self-organized percolation method that allows us to obtain the critical value of the percolation parameter in a single run, for a given network. We consider a parallel SIS process, which is equivalent to a directed percolation problem where the directed direction is time. Let us denote by $x_i(t) = 0,1$ ($0 =$ healthy, $1 =$ infected) the percolating variable and by p the control parameter (percolation probability).

A. Simple infection (direct percolation)

Assuming that the infection probability τ is fixed, the stochastic evolution process for the network is defined as

$$x_i(t+1) = \bigvee_{j=j_1^{(i)},\ldots,j_{k_i}^{(i)}} [\tau > r_{ij}(t)] x_j(t), \tag{8}$$

where $\bigvee$ represents the OR operator and the multiplication operation is to be replaced by the AND logical operation. The brackets represent the truth function, $[\cdot] = 1$ if "$\cdot$" is true and 0 otherwise. The quantity $r_{ij}(t)$ is a random number between 0 and 1, drawn independently for each triplet i,j,t. We want to derive an equation for $\tau_i(t)$, which is the minimum value of τ for which $x_i(t)$ is infected. We can replace $x_i(t)$ with $[\tau > \tau_i(t)]$. Equation (8) becomes

$$[\tau > \tau_i(t+1)] = \bigvee_{j=j_1^{(i)},\ldots,j_{k_i}^{(i)}} [\tau > r_{ij}(t)][\tau > \tau_j(t)]. \tag{9}$$

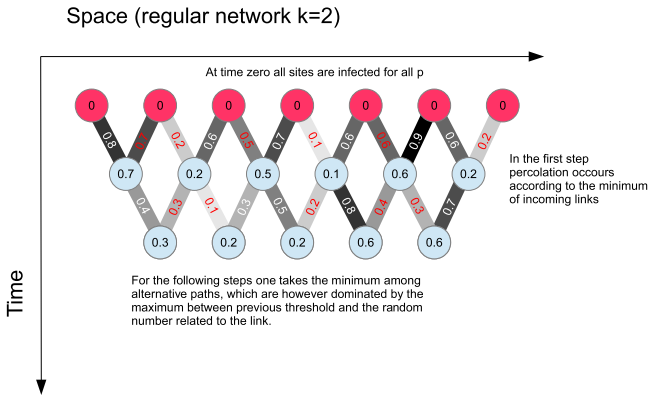

FIG. 4. (Color online) Evolution of the local minimum value of the percolation parameter p_i for a 1D regular network with $k = 2$.

Now $[\tau > a][\tau > b]$ is equal to $[\tau > \max(a,b)]$ and $[\tau > a] \vee [\tau > b]$ is equal to $[\tau > \min(a,b)]$. Equation (9) becomes

$$[\tau > \tau_i(t+1)] = \left[\tau > \left(\min_{j=j_1^{(i)},\ldots,j_{k_i}^{(i)}} \max(r_{ij}(t), \tau_j(t))\right)\right], \tag{10}$$

and we get the desired equation for the τ_i's:

$$\tau_i(t+1) = \min_{j=j_1^{(i)},\ldots,j_{k_i}^{(i)}} \max(r_{ij}(t), \tau_j(t)). \tag{11}$$

Let us assume that at time $t = 0$ all sites are infected, so that $x_i(0) = 1\ \forall\tau$. We can alternatively write $\tau_i(0) = 0$, since the minimum value of τ for which $x_i(0) = 1$ is 1 for sure. We can iterate Eq. (11) and get the asymptotic distribution of τ_i. The minimum of this distribution gives the critical value τ_c, for which there is at least one percolating cluster with at least one "infected" site at long times. As usual, t cannot be infinitely large for finite N; otherwise, there will surely be a fluctuation that will bring the system into the absorbing (healthy $x_i = 0$) configuration. A schematic of this modus operandi is shown in Fig. 4.

B. Infection with risk perception

Now let us apply the method to a more difficult problem, for which the percolation probability depends on the fraction of infected sites in the neighborhood (risk perception), as expressed by Eq. (1). In this case we want to find the minimum value of the parameter J for which there is no spreading of the infection at long times. The quantity $[u > r] = [\tau \exp(-Js/k) > r]$ is equivalent to $[J < -(k/s)\ln(r/\tau)]$. Therefore Eq. (9) is replaced by

$$[J < J_i(t+1)] = \bigvee_{j=j_1^{(i)},\ldots,j_{k_i}^{(i)}} \left[J < -\frac{k_i}{s_i} \ln\left(\frac{r_{ij}(t)}{\tau}\right)\right] \times [J < J_j(t)], \tag{12}$$

where

$$s_i \equiv s_i(J) = \sum_{j=j_1^{(i)},\ldots,j_{k_i}^{(i)}} x_j = \sum_{j=j_1^{(i)},\ldots,j_{k_i}^{(i)}} [J_j(t) \geqslant J]. \tag{13}$$

So

$$[J < J_i(t+1)] = \bigvee_{j=j_1^{(i)},\ldots,j_{k_i}^{(i)}} \left[J < -\frac{k_i}{s_i(J_j(t))} \ln\left(\frac{r_{ij}(t)}{\tau}\right)\right] \times [J < J_j(t)], \tag{14}$$

and therefore

$$J_i(t+1) = \max_{j=j_1^{(i)},\ldots,j_{k_i}^{(i)}} \min\left(-\frac{k_i}{s_i(J_j(t))} \ln\left(\frac{r_{ij}(t)}{\tau}\right), J_j(t)\right). \tag{15}$$

Analogously to the previous case, the critical value of J_c is obtained by taking the maximum value ofe $J_i(t)$ for some large (but finite) value of t.

C. The self-organized percolation method for multiplex networks

We can now turn to the problem of computing the critical value J_c for a fixed value of τ if the perception is computed for the information network which is partially different from the physical one, where infection spreads. Here the perception of the importance of the infection, $\bar{s}_i$, is computed for the neighbors $\bar{j}^{(i)}$ in the information network. The perceived number of infected neighbors depends on how many of them, in the information network, have a $J_{\bar{j}}$ value larger than that computed in the physical network; i.e.,

$$J_i(t+1) = \max_{j=j_1^{(i)},\ldots,j_{k_i}^{(i)}} \min\left(-\frac{k_i}{\bar{s}_i(J_j)} \ln\left(\frac{r_{ij}(t)}{\tau}\right), J_j(t)\right), \tag{16}$$

where

$$\bar{s}_i(J_j) = \sum_{\bar{j}=\bar{j}_1^{(i)},\ldots,\bar{j}_{k_i}^{(i)}} [J_{\bar{j}} \geqslant J_j]. \tag{17}$$

In other words, for a given site i, one has to consider its neighbors j with parameter J_j. For each value J_j one computes how many neighbors $\bar{s}_i(J - j)$ in the *information* network ($\bar{j}_i$) have $J_{\bar{j}} \geqslant J_j$. This allows us to establish the contribution to the minimum precaution level J_i coming from neighbor j which is infected if $J \leqslant J_j$.

V. RESULTS

In this section we report the results of the self-organized percolation method in both single-layered and multiplex networks (with and without risk perception). For our experiments we generally use the network size $N = 10\,000$ and the computational time $T = 10\,000$ time steps.

A. Percolation in single-layered networks (SIS dynamics)

We investigated SIS dynamics over regular, Poisson, and scale-free networks as shown in Fig. 5. In particular, we evaluated the critical epidemic threshold values τ_c for which there is at least one percolating cluster with at least one infected node (points labeled "Theory τ_c" in Fig. 5).

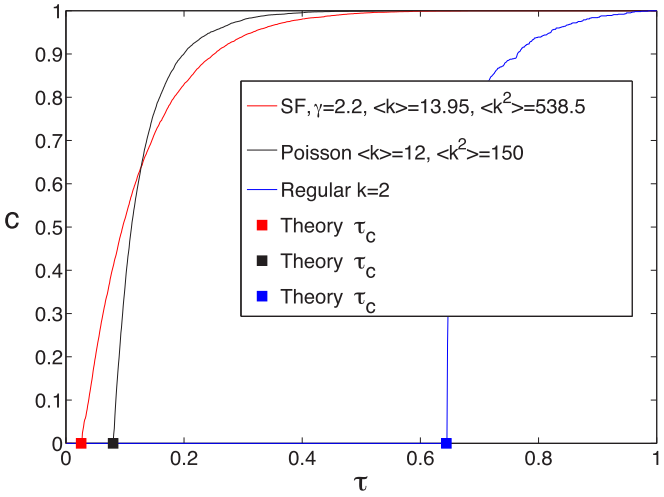

FIG. 5. (Color online) Asymptotic number of infected individuals c versus the bare infection probability τ for the SIS dynamics for different networks. From left to right, for $c = 0$: scale-free (SF), random (Poisson), and regular. Here $N = 10\,000$.

Considering a regular lattice with connectivity degree $k = 2$, we found $\tau_c \simeq 0.6447$, which is compatible with the results of the bond percolation transition in the Domany-Kinzel model [28]. In the case of random networks with Poisson degree distributions the critical epidemic threshold $\tau_c = \langle k\rangle/\langle k^2\rangle \simeq \langle k\rangle^{-1}$ if the distribution is sharp [5]. Indeed, for a Poisson network with $\langle k\rangle = 12$ the self-organized percolation method gives $\tau_c \simeq 0.08 \simeq 1/12$. For a scale-free network with $\langle k\rangle = 13.95$ and $\langle k^2\rangle = 538.5$, from simulations we get $\tau_c \simeq 0.026$, in agreement with the expected value.

B. Effects of risk perception in SIS dynamics

We investigate the effects of risk perception in the previous simple model of epidemic spreading. The results are quite interesting compared with the simple SIS dynamics. By inserting the risk perception it is possible to stop the epidemic for every value of the bare infection probability τ up to $\tau = 1$. Let us consider, for instance, the case of random networks with $\langle k\rangle = 6$. For the simple infection process we found a critical value $\tau_c = 0.165$. As shown in Fig. 2, beyond this value of τ_c the epidemic can still be stopped if all agents adopt a sufficiently high precaution level J. The same consideration can be applied also for the other scenarios (Fig. 3).

C. Multiplex risk perception

The phase diagram for the risk perception with SIS dynamics in multiplex networks is shown in Fig. 6. The general shape of this phase diagram can be understood by considering that a given node of physical connectivity k_r is connected, in the information network, to $(1 - q)k_r$ physical neighbors, the rest being virtual ones. At the threshold, the global fraction of infected sites is small. For the spreading of the epidemic, the important sites are those that have an infected physical

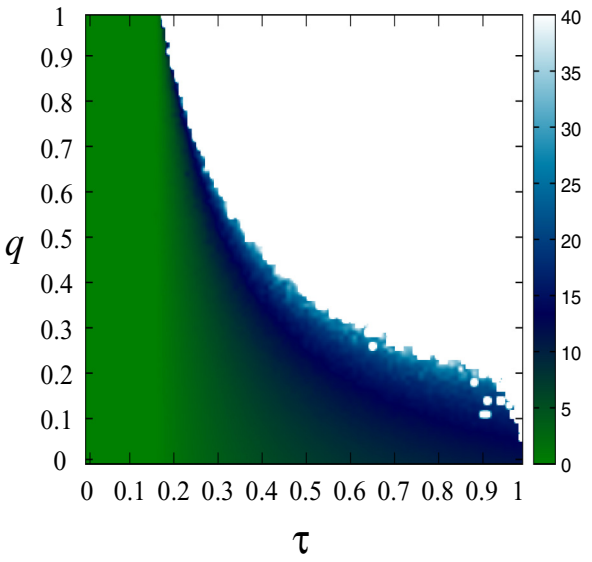

FIG. 6. (Color online) Critical precaution threshold J_c (gray intensity or color code) as a function of the bare infection τ and of the difference q between the physical and the information network. Here the physical and virtual networks are Poissonian (random), with $\langle k \rangle = 6$ and $N = 1000$. In the darker region there is always a value of J_c able to stop the epidemic, while in the white region the epidemic cannot be stopped.

neighbor. It may be assumed that the virtual neighbors, being uncorrelated with the physical ones, do not contribute at all to the risk perception. Among the physical neighbors, the fraction qk_r, replaced by virtual ones, has become invisible, and so the perception decreases by a factor q. For a given

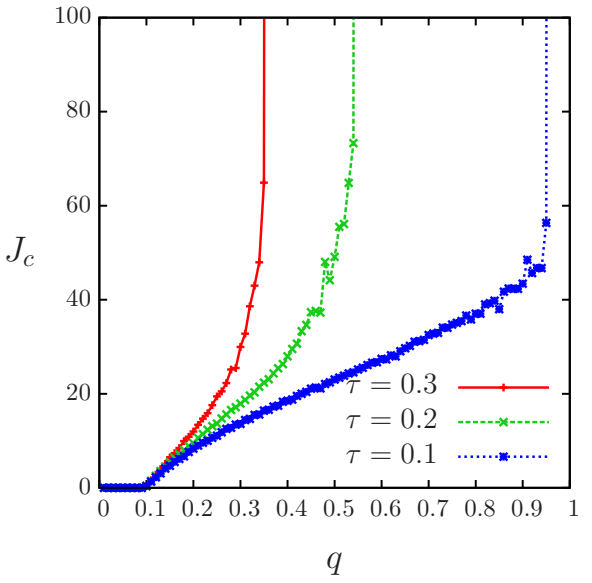

FIG. 7. (Color online) Critical precaution threshold J_c versus the difference between the physical and the information network q for some values of the bare infection τ (from right to left $\tau = 0.1$, 0.2, 0.3). Random physical network and scale-free virtual network, both with $\langle k \rangle = 6$, $N = 10\,000$.

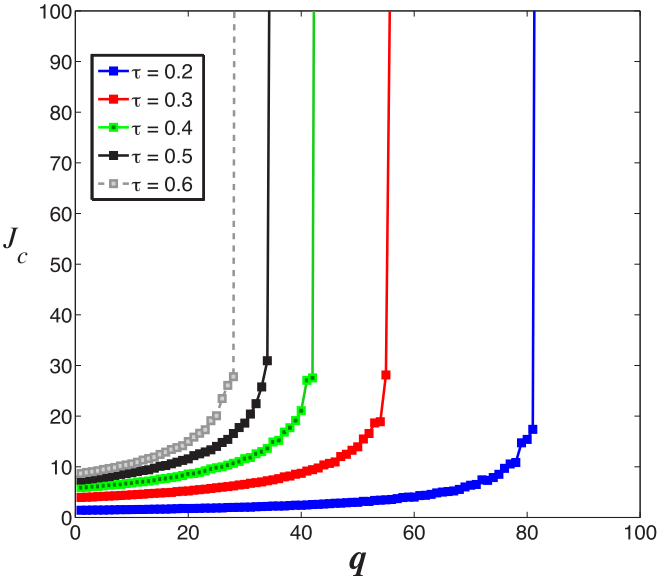

FIG. 8. (Color online) Critical precaution threshold J_c versus the difference between the physical and the information network q for some values of the bare infection τ (from right to left: $\tau = 0.2, 0.3, \ldots, 0.6$). Random physical and virtual networks, both with $\langle k \rangle = 6$ and $N = 10\,000$.

value of the perception, the infection is stoppable only if the infectiousness is also decreased by a factor q. Indeed, the shape of the stoppability boundary in Fig. 6 resembles that of a hyperbola $\tau q = \text{const}$. Note, however, that near $\tau = 1$ stopping the spread appears to be almost impossible, even for small values of q. Indeed, simulations with $N = 10\,000$ show that for $\tau = 1$ the critical value of q that gives a finite value of J_c is very close to 0. This is probably due to the formation of a core of nodes connected by "invisible" links. If two or more sites are mutually connected at the physical level but not at the information level, and all their physical neighbors are healthy, their perception of the risk is null. For $\tau = 1$ they may keep infecting each other, while not propagating the disease to the other neighbors that have information about their ill state, since, if J is large, the effective infection probability in the presence of risk perception is vanishing.

The general trend is that, with an increase in the difference q between the information network and the physical one, it becomes harder to stop an epidemic. It is interesting to investigate this transition. As we can see in Fig. 7 for a physical random and virtual scale-free network, this transition is quite sharp, especially for low values of τ. A similar scenario holds for a mixture of physical and virtual random networks, as shown in Fig. 8.

VI. CONCLUSIONS

We have investigated the interplay between epidemic spreading and risk perception in multiplex networks, exploiting mean-field approximations and a self-organized method that automatically gives the percolation threshold in just one simulation. We have focused on multiplex networks, considering that people get infected by physical contacts in

real life but often gather information from an information network, that which be quite different from the physical ones. The main conclusion is that the similarity between the physical and the information networks determines the possibility of stopping the infection for a sufficiently high precaution level: if the networks are too different, there is no means of avoiding the epidemic. Moreover, especially for low values of the bare infection probability, this transition occurs sharply, without evident forerunners. The sudden occurrence of this transition constitutes a warning against relying too much on the Internet as the sole source of information: although the virtual world indeed has the advantage of allowing rapid diffusion of information, real epidemics still propagate in the physical world. This is of particular importance for those diseases, possibly diffused in a marginalized part of the population or in some ethnic group, that do not reach the media level. In the present society, it is quite possible that people from different social levels establish a "physical" contact (and thus the possibility of contagion) even if they are not in contact at the "information" level.

ACKNOWLEDGMENTS

The authors are grateful to Dr. Nicola Perra for helpful discussions. F.B. acknowledges partial financial support from European Commission (ICT-20111.1.6) Proposal No. 288021 EINS - Network of Excellence in Internet Science and European Commission (FP7-ICT-2013-10) Proposal No. 611299 SciCafe 2.0.

[1] Pandemic scares throughout history. HealthMag. http://www.health.com/health/gallery/0,,20307381,00.html (2013).
[2] http://en.wikipedia.org/wiki/Pandemic (2013).
[3] F. Macrae, The "false" pandemic: Drug firms cashed in on scare over swine flu, claims Euro health chief. Daily Mail, http://www.dailymail.co.uk/news/article-1242147/The-false-pandemic-Drug-firms-cashed-scare-swine-flu-claims-Euro-health-chief.html (2010).
[4] C. Moore and M. E. J. Newman, Phys. Rev. E **61**, 5678 (2000).
[5] R. Pastor-Satorras and A. Vespignani, Phys. Rev. Lett. **86**, 3200 (2001).
[6] M. E. J. Newman, SIAM Rev. **45**, 167 (2003).
[7] R. M. May and A. L. Lloyd, Phys. Rev. E **64**, 066112 (2001).
[8] R. Pastor-Satorras and A. Vespignani, Phys. Rev. E **65**, 036104 (2002).
[9] http://en.wikipedia.org/wiki/Lazaretto (2013).
[10] R. J. Palmer, *L'azione della repubblica di Venezia nel controllo della peste. Lo sviluppo della politica governativa, Venezia e la peste 1348-1797* (Marsilio Editori, Venice, 1979).
[11] F. Bagnoli, P. Liò, and L. Sguanci, Phys. Rev. E **76**, 061904 (2007).
[12] J. Ginsberg, M. Mohebbi, R. Patel, L. Brammer, M. Smolinski, and L. Brilliant, Nature **457**, 1012 (2009).
[13] D. Scanfeld, V. Scanfeld, and E. L. Larson, Am. J. Infect. Control **38**, 182 (2010).
[14] C. Chew and G. Eysenbach, PLoS ONE **5**, e14118 (2010).
[15] The state of the news media. The Pew Research Center's project for excellence in journalism, http://stateofthemedia.org/ (2014). In particular: "What Facebook and Twitter Mean for News" http://www.stateofthemedia.org/2012/mobile-devices-and-news-consumption-some-good-signs-for-journalism/what-facebook-and-twitter-mean-for-news/ (2012) and "Friends and Family - Important Drivers of News" http://www.stateofthemedia.org/2013/special-reports-landing-page/friends-and-family-important-drivers-of-news/ (2013).
[16] M. Kurant and P. Thiran, Phys. Rev. Lett. **96**, 138701 (2006).
[17] P. J. Mucha, T. Richardson, K. Macon, M. A. Porter, and J.-P. Onnela, Science **328**, 876 (2010).
[18] M. Szell, R. Lambiotte, and S. Thurner, Proc. Natl. Acad. Sci. USA **107**, 13636 (2010).
[19] J. Gómez-Gardeñes, I. Reinares, A. Arenas, and L. M. Floría, Sci. Rep. **2**, 620 (2012).
[20] G. Bianconi, Phys. Rev. E **87**, 062806 (2013).
[21] S. V. Buldyrev, R. Parshani, G. Paul, H. E. Stanley, and S. Havlin, Nature **464**, 1025 (2010).
[22] J. Gao, S. V. Buldyrev, H. E. Stanley, and S. Havlin, Nat. Phys. **8**, 40 (2012).
[23] C. Granell, S. Gómez, and A. Arenas, Phys. Rev. Lett. **111**, 128701 (2013).
[24] C. Granell, S. Gómez, and A. Arenas, Phys. Rev. E **90**, 012808 (2014).
[25] F. Bagnoli, P. Palmerini, and R. Rechtman, Phys. Rev. E **55**, 3970 (1997).
[26] S. N. Dorogovtsev and J. F. F. Mendes, Adv. Phys. **51**, 1079 (2002).
[27] R. Pastor-Satorras and A. Vespignani, Phys. Rev. E **65**, 035108(R) (2002).
[28] E. Domany and W. Kinzel, Phys. Rev. Lett. **53**, 311 (1984).